INSTITUTE OF PHYSICS PUBLISHING NANOTECHNOLOGY
Nanotechnology **17** (2006) 622–633 doi:10.1088/0957-4484/17/3/002

Simulation of the electric response of DNA translocation through a semiconductor nanopore–capacitor

Maria E Gracheva[1], Anlin Xiong[1], Aleksei Aksimentiev[2], Klaus Schulten[2], Gregory Timp[1] and Jean-Pierre Leburton[1,3]

[1] Department of Electrical and Computer Engineering, University of Illinois at Urbana-Champaign, Urbana, IL 61801, USA
[2] Department of Physics, University of Illinois at Urbana-Champaign, Urbana, IL 61801, USA

E-mail: gracheva@uiuc.edu and jleburto@uiuc.edu

Received 18 October 2005, in final form 29 November 2005
Published 6 January 2006
Online at stacks.iop.org/Nano/17/622

Abstract
A multi-scale/multi-material computational model for simulation of the electric signal detected on the electrodes of a metal–oxide–semiconductor (MOS) capacitor forming a nanoscale artificial membrane, and containing a nanopore with translocating DNA, is presented. The multi-scale approach is based on the incorporation of a molecular dynamics description of a translocating DNA molecule in the nanopore within a three-dimensional Poisson equation self-consistent scheme involving electrolytic and semiconductor charges for the electrostatic potential calculation. The voltage signal obtained from the simulation supports the possibility for single nucleotide resolution with a nanopore device. The electric signal predicted on the capacitor electrodes complements ongoing experiments exploring the use of nanopores in a MOS capacitor membrane for DNA sequencing.

(Some figures in this article are in colour only in the electronic version)

1. Introduction

In the middle of the 1990s, single molecule translocation through a proteinaceous nanopore was proposed as a new tool for DNA characterization [1]. Single stranded DNA molecules have a diameter of 1–2 nm [2], which is comparable to the pore size of biological ion channels [3]. It was suggested that by utilizing the natural nanoscale features of a proteinaceous pore, one can obtain direct information on the DNA molecular structure. Indeed, when an electric field drives a DNA molecule through the proteinaceous nanopore in a lipid bilayer placed in an electrolyte solution, the DNA molecule partially or totally blocks the pore, reducing the ionic current through it. Hence, the passage of each DNA molecule can be detected as a transient decrease of ionic current whose duration is proportional to the DNA length. Many experiments have been done in this context [1, 4–10] demonstrating how the length of the DNA chain is related to the time of the ionic current blockade. Later works revealed additional factors, such as temperature [5], driving voltage (applied electric field) [9], and DNA pairing [4, 6, 7, 10], affecting the DNA translocation rate. Moreover, in the case of mono-nucleotide chains, this technique has been able to discriminate between polymers of different molecular compositions [4, 6, 10].

Although proteinaceous nanopores are convenient DNA characterization tools, they have shortcomings as the pore is of a fixed size, and its stability and low noise characteristics are restricted to well defined chemical, mechanical, electrical and thermal conditions [11]. In recent years, artificial solid-state nanopores made of silicon and silicon compounds began to replace the original bio-nanopores, and promise to overcome limitations of the latter [11–15]. As with

[3] Author to whom any correspondence should be addressed.

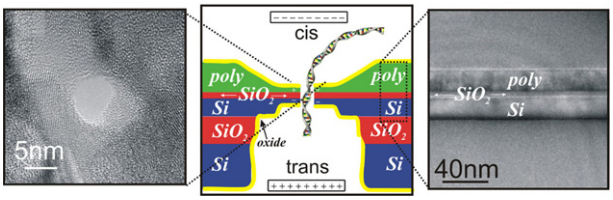

Figure 1. Centre panel: schematic diagram of a novel biosensor consisting of a nanopore in a capacitor membrane. Right panel: high-resolution TEM image through the capacitor membrane structure. Left panel: high-resolution lattice image of a nanopore sputtered into the capacitor membrane.

proteinaceous nanopores, the correlation between DNA translocation and ionic current blockage has been established by both simulations and experiments [13, 16, 17]. By measuring the duration and magnitude of the blocking current transient, the polymer length of single-stranded DNA (ssDNA) can be determined [13]. However, for both bio-nanopore and solid-state nanopore systems, complete characterization of DNA molecules is still at its early stage. Nevertheless, quoting our colleagues: 'with further improvements, the method could in principle provide direct, high-speed detection of the sequence of bases in single molecules of DNA or RNA' [1].

In this paper, we describe a novel solid-state device, a nanopore in a membrane fabricated from a metal–oxide–semiconductor (MOS) capacitor, that can be used to electrically detect DNA. As a DNA molecule is forced to translocate through the nanopore by an externally applied bias voltage the electronic signature of the molecule is recorded in the form of a voltage trace on the capacitor plates/electrodes. Following a preliminary demonstration, we have developed a computational model that simulates the electrical response of DNA translocation through a nanopore in a SiO_2 membrane sandwiched between two conducting layers of heavily doped Si (figure 1 (centre panel)). We show that the new device has the potential to identify DNA molecules by using the voltage induced on the electrodes without utilizing the signal of ionic current fluctuations.

2. Motivation: device structure description

A synthetic nanopore in a MOS capacitor is schematically illustrated in figure 1 (centre panel). It consists of a very thin (<5 nm) SiO_2 membrane, sandwiched between two heavily doped silicon layers (one polycrystalline silicon; the other crystalline silicon) sitting on a thicker oxide layer, and covered by a thin oxide layer. A nanopore of diameter smaller than or equal to 2 nm is etched through the membrane layers in the thinnest (centre) part of the structure. The details of the fabrication process are described elsewhere [14]. The whole structure is immersed in a KCl buffer solution containing two external electrodes under electric bias, which can also measure the ionic current flowing through the nanopore, as proposed in other DNA molecule detectors [4, 10, 14].

The device membrane forms a nanoscale electric capacitor, which can record voltage fluctuations induced by the sequence of charges carried by a DNA strand when it translocates through the nanopore. This solid-state device has several advantages over a proteinaceous pore. The primary advantage is the four-terminal measurement configuration and the high spatial resolution that can be achieved by using a thin gate oxide. There are several substantial differences from previous work. All prior transmembrane current detection schemes detect a blockade in the current through a proteinaceous or synthetic pore in a membrane 5–100 nm thick encompassing 20–300 bases using a two-terminal measurement. In contrast, our detection strategy, illustrated by the schematic diagram shown in figure 1, uses a four-terminal measurement configuration to sense the voltage across a dielectric that can be as thin as 0.7 nm. We have shown (see figure 2) that we can detect the voltage associated with a DNA molecule translocating between the two electrodes comprising the capacitor. The data shown in figure 2 represent the voltages observed on the two electrodes when ssDNA permeates a 7.0 nm diameter pore in an MOS–capacitor membrane. To the best of our knowledge this has never been done before. Furthermore, the thickness of the dielectric, which essentially determines the spatial resolution of the voltage measurement, can be controlled with subnanometre precision. On the other hand, the resolution of the current blockade measurements using proteinaceous pores is determined by the 5–8 nm thickness of the phospholipid membrane. An additional advantage of our method is that the diameter of the pore, a crucial parameter, can be controlled with subnanometre precision. In particular, a 1 nm diameter pore is required to constrain the lateral motion of a ssDNA molecule, to force the orientation of the bases along the pore axis, and to exclude solution from the pore which screens the signal associated with the partial charges on the molecule. Indeed, we have demonstrated already the facility for fabricating 1 nm pores and have shown data of ssDNA translocating through it, a crucial prerequisite for the practical implementation of the MOS–capacitor–nanopore sensor. For this purpose we plan to use capacitor membranes with an area of only 2 μm by 2 μm. The biological membranes used for the blockade experiments are 100–1000 times larger. The smaller membrane reduces the capacitance and facilitates high-frequency measurements. Also it is possible to use the electrodes to directly detect a translocation by measuring the time delay between the voltage response on each electrode.

The use of semiconductor materials allows also direct integration of nanoscale MOS amplifiers with high sensitivity on the nanopore layer structure to improve the voltage signal. Owing to the short distance between the two capacitor plates, one can expect the voltage signal to be characteristic of the electronic structure of the DNA molecule, potentially with resolution up to a single base pair when the capacitor dielectric and nanopore diameter are $\sim$1 nm. Because of the solid-state nature of the nanopore, the system is robust. It operates over a wide range of electrolyte concentrations, pH [18], temperature and external voltages [19], unlike proteinaceous pores that operate under stringent chemical and electrical conditions. This last consideration provides wide latitude to optimize the system for better detection.

The membranes are manufactured using conventional semiconductor processing techniques, starting with a 200 mm semiconductor–oxide–insulator (SOI) wafer with a silicon

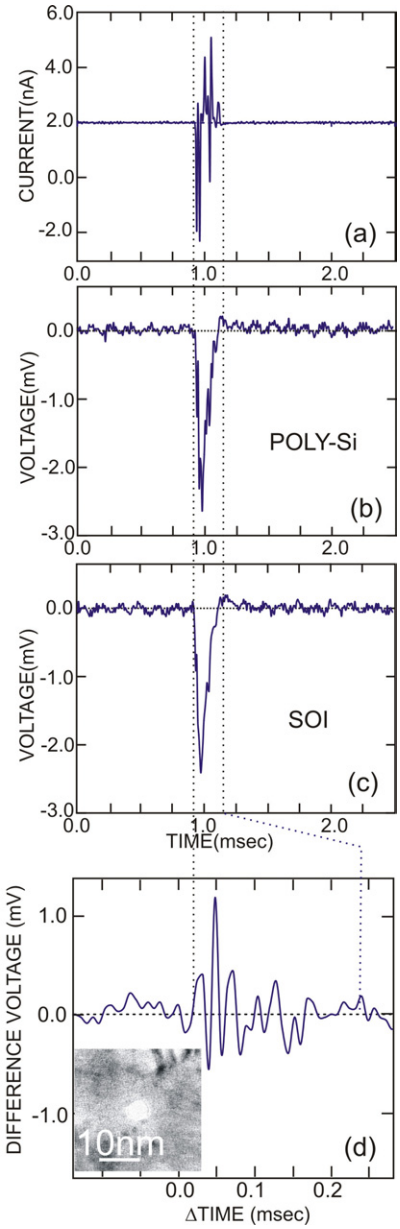

Figure 2. Translocation through a 7 nm diameter pore in a capacitor. Corresponding to a transient in the current (a), we observe a voltage signature on the SOI and poly-silicon electrodes (b) and (c) respectively. We attribute these signals to the translocation of a DNA through the pore. (d) Shows the difference between the poly and SOI electrodes. A STEM image of the 7 nm diameter pore is shown in the inset of (d).

layer 20 nm thick on a 150 nm thick buried oxide. Rapid thermal oxidation of the heavily doped (n-type or p-type) crystalline silicon (SOI) layer is used to produce a high-integrity gate dielectric <5 nm thick. Subsequently, heavily doped poly-silicon is deposited on the oxide and chemical–mechanical polishing is used to reduce the thickness of the poly electrode to about 20 nm (see figure 1 (centre panel)). A high-resolution transmission electron microscope (TEM) cross-section image through the membrane structure is shown in figure 1 (right panel). A membrane, comprised of the poly-SiO_2–silicon capacitor, is formed by creating a through-wafer by using optical lithography in conjunction with reactive ion and wet chemical etching on sacrificial layers. After electrical contacts to the top and bottom silicon electrodes are formed, a nanopore is produced in the membrane using a tightly focused, high-energy electron beam to sputter atoms from the capacitor. A top-down lattice image of the 6–7 nm diameter pore through the membrane is shown in figure 1 (left panel). The figure shows a TEM image of an $R_p = 3.5 \pm 0.1$ nm radius pore produced in a poly-SiO_2–silicon membrane 45 nm thick, taken at a tilt angle of 0°. This image represents a two-dimensional (2D) projection through the membrane. The shot noise observed in the area identified as the pore is indicative of perfect transmission of the electron beam through the pore in the membrane. The three-dimensional (3D) structure can be inferred from 2D projections of the pore taken at various tilt angles. Although it is not unique, one simple model for the structure consists of two intersecting cones each with a cone angle of ∼30° in this case. To ensure the integrity of the capacitor, we measured the tunnelling current between the electrodes prior to and after the pore had been sputtered [14, 17].

As a preliminary assessment of the nanopore–capacitor sensor, we attempted to detect the translocation of a single DNA molecule. While smaller pores have been produced in capacitor membranes [17], we attempted to detect the translocation of a single DNA molecule in the 7 nm diameter pore shown in the inset to figure 2 to assess the size of the signal. The signal level observed under these conditions is expected to be a lower bound since it may be reduced by screening due to electrolyte in the pore. First, we measured the dc electrolytic current through a single pore as a function of the applied electrochemical potential at 23.5 ± 1 °C in a membrane transport bi-cell made of acrylic. Each cell contained a volume of KCl electrolyte ranging from 75 μl to ∼1 ml, and a Ag–AgCl electrode positioned ∼1 mm from the membrane. A constant voltage bias was applied between the electrodes and then the steady-state current was measured using an Axopatch 200B amplifier with a 10 kHz bandwidth. Subsequently, we injected DNA along with TRIS-EDTA buffer (pH 8.0) into 1 M KCl electrolyte near the negative electrode. While monitoring the ionic current through the pore under an applied bias, we observed transients associated with single DNA molecules temporarily blocking the electrolytic current through the pore [17].

Figure 2(a) shows a continuous time sequence of the current through a pore of radius $R_p = 3.5$ nm observed for an applied bias of 200 mV after injecting 150 bp double-stranded DNA (dsDNA) at the negative electrode, illustrating a single current transient superimposed on the dc electrolytic current. We have previously reported that field-driven translocations of the DNA cause a temporary blockade of the open current through the pore [17]. However, the narrow bandwidth (100 kHz) of the amplifier precludes the observation of transients associated with interactions between the pore and the molecule that are shorter than 10–100 μs. Concomitant with the observation of the current transient, we observe transients in the voltage signal on the poly-Si and c-Si electrodes. Figures 2(a)–(d) represent simultaneous measurements of the current through the pore (a), the voltages on the poly (b), and c-Si electrode (c), and the difference voltage (d) that

was nearly coincident with an event observed in the current (a). We attribute these signals to the translocation of a single DNA molecule through the pore. The voltage signal associated with the translocation is on the level of ∼1 mV with a duration of about 200 μs. Figure 2(d) presents the difference voltage measured between the SOI and poly-silicon electrodes, showing a >1 mV zero-to-peak signal level above a noise background of about 0.1 mV rms. The fluctuations observed in the difference voltage with about a 25 μs period are comparable to the response time associated with the 50 kHz bandwidth of the Axon 700B amplifier used for the voltage measurements. This difference voltage signal provides us with an unequivocal identification of a translocation event since both probes show a voltage signature. While we frequently observe a signal on the poly electrode on the *cis* side of the membrane, we do not always observe a signal on the SOI electrode on the *trans* side. This is in contrast with all previous work on nanopores in which the current transients were tentatively categorized by analysing the duration as well as the percentage blockage of the current either as DNA translocations through the pore or as a 'bounce' reflecting unsuccessful attempts of the DNA to transit across the membrane. This interpretation is dubious since the duration and percentage blockade current depend on the initial configuration of the molecule relative to the pore [16]. Also in [16] we discuss issues related to DNA concentration and frequency of DNA translocation events.

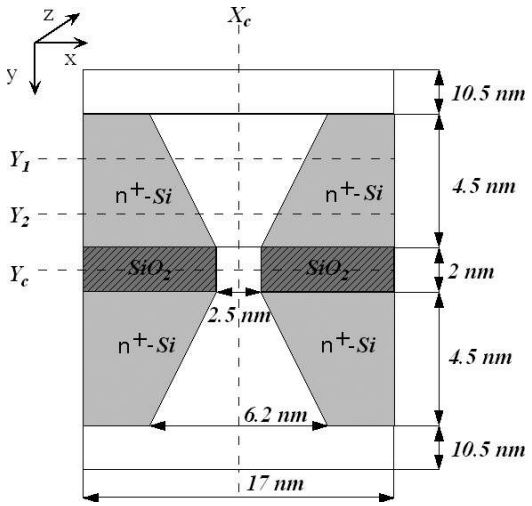

Figure 3. Schematic diagram of the device geometry: the xy cross-section through the centre of the nanopore (the yz cross-section is similar) provides a side view of the modelled device and cross-sections for which the electron, negative and positive ion concentrations are represented in the following figures. The drawing is not to scale.

3. Modelling

In order to achieve an understanding of the electrostatics at play between the different materials, i.e. the electrolytic solution and the DNA molecules interacting with the semiconductor/oxide structure, we have developed a computational model of the device that reproduces realistically the bio-electronic system shown in figure 1(a). In our model the top poly-Si and bottom Si capacitor films have been replaced by two heavily doped n^+-Si layers. The nanopore is placed in the centre of the membrane and is assumed to have cylindrical symmetry. The n^+-Si layers have conical shape above and below the nanopore as a result of the electron beam sputtering.

A schematic diagram of the idealized device geometry is shown in figure 3. We denote several cross-sections, one vertical (X_c) and three horizontal (Y_1, Y_2, Y_c), for which the concentrations of electrons and K^+/Cl^- ions are shown in the following figures. Besides the central cross-sections (X_c and Y_c) there are two horizontal ones (Y_1, Y_2) across the structure. We chose the coordinate system in which the y-axis is parallel to the nanopore axes and the xz plane is parallel to the device structure layers including the SiO_2 layer.

3.1. Multiscale approach

The duration of a DNA translocation through a synthetic nanopore depends on the diameter of the pore, the thickness of the membrane, the electric field, the orientation and conformation of the molecule, the interaction between DNA and the pore, the reduction of the driving force by the counter-ion condensation, which in turn reduces the DNA effective charge, and on the hydrophobic adhesion of bases to the pore surface. On a timescale of 10 ns, hydrophobic adhesion is the predominant force affecting the duration of the translocation of ssDNA and RNA strands when the diameter of the pore is larger than the diameter of the strand. From molecular dynamics simulations [16] we estimated that, if counter-ion condensation predominates over steric friction, then at a 1 V bias the translocation velocity should not exceed 1 nucleotide/10 ns (∼0.03 nm ns^{-1}). This speed is almost two orders of magnitude slower than the velocity observed when the steric constraints are applied to DNA atoms only. On the other hand, it is anticipated that the RC time constant associated with the measurement of the voltage on a 2 μm by 2 μm capacitor with a 2 nm thick gate oxide ($C \sim 40$ fF) is about ∼1 ns.

We conclude that for each DNA molecule conformation in the nanopore, the nanocapacitor reaches its electrostatic steady state quickly, which implies that the electric capacitor can easily follow the corresponding charge motion of the DNA strand through the nanopore.

To start our analysis, we assume a quasi-static behavior of electrical response, and consider a step-by-step motion of DNA through the nanopore. For each DNA position in the nanopore we compute the voltage response on the capacitor electrodes self-consistently. For this purpose we use a multiscale approach, in which the DNA translocation through the nanopore is simulated by molecular dynamics while the voltage response in the solid-state capacitor is modelled by a 3D self-consistent Poisson Solver (PS) incorporating the charge variation in the electrolytic solution as well as in the semiconductor materials and the oxide.

3.2. Molecular modelling of DNA translocation through a solid-state nanopore

Molecular dynamics (MD) provides an atomic-level description of the DNA translocation through synthetic nanopores. In this method, a molecular system is approximated by an ensemble of atoms interacting with each other according to a molec-

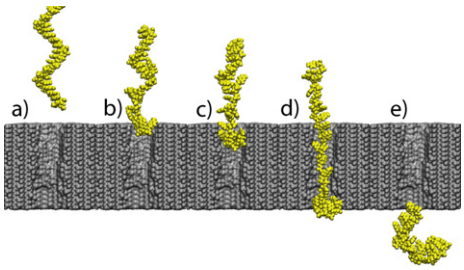

Figure 4. Molecular dynamics simulation of DNA translocation through the pore. (a) The starting conformation (water and ions are not shown). (b) Capture of the DNA strand by the pore. (c) DNA entering the pore. (d) Translocation. (e) Exit from the pore.

ular force field that has been developed and calibrated to reproduce quantitatively the physical properties of the simulated system. The methodology of MD simulations of DNA/nanopore systems has been described in detail elsewhere [16, 20]; here, we demonstrate the method by one illustrative example.

Figure 4(a) shows a microscopic model of a DNA/nanopore systems comprising 35 000 atoms. By removing atoms from a crystalline Si_3N_4 membrane, a double-conical pore was created, complying with the geometry of the pores manufactured in Si_3N_4 by a highly focused, bright electron beam [13]. A homopolymer of 20 cytosine nucleotides poly$(dC)_{20}$ was placed in front of the pore. The pore and the DNA strand were submerged in a volume of pre-equilibrated water molecules; potassium and chlorine ions were added corresponding to a concentration of 1 M. In order to perform MD simulations on a DNA/nanopore system, a molecular force-field describing water, ions and nucleic acids [21] was combined with the MSXX force-field developed for a Si_3N_4 [22]. A uniform electric field was applied to every charged atom in the system, inducing, at the beginning of the simulation, a rearrangement of the ions, which focused the electric field to the vicinity of the membrane, abolishing the field gradient in the bulk. In a 2 ns simulation, we observed the capture (figure 4(b)) and the subsequent translocation (figures 4(c)–(e)) of the DNA strand through the pore. As the DNA strand transits the pore, we collect snapshots of the DNA conformation, which, together with the partial charges provided by the AMBER95 force field, can be used to compute the self-consistent electrostatic potential inside the nanopore sensor.

3.3. 3D self-consistent modelling of the capacitor response

By tracking the motion of every atom in the DNA strand during its translocation, molecular dynamics provides the temporal charge distribution of the polymer in the nanopore. In future work we plan to use the molecular charge distribution for a sequence of 'snapshots' of the DNA conformations in a continuum charge model of the electrolyte and the solid-state materials to compute the electrostatic potential in the whole region, and specifically in the Si layers, to obtain the voltage response due to DNA translocation. In this paper we are testing our model with only one snapshot of initial DNA charge distribution that we rigidly move through the pore.

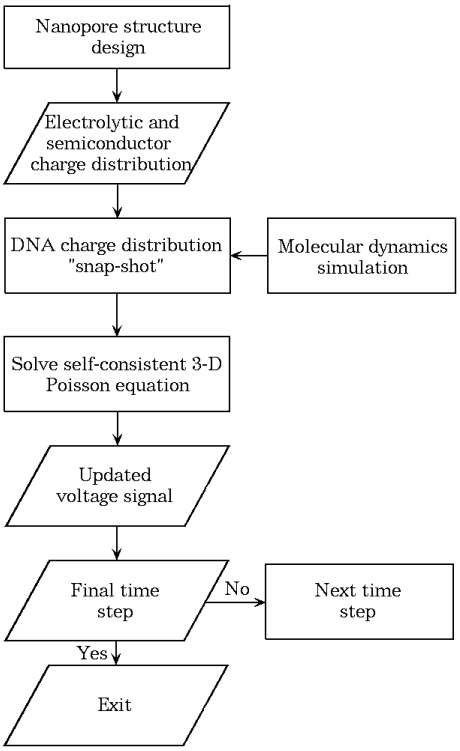

Figure 5. Chart diagram of the proposed multi-scale approach to calculation of the electrostatic charge and potential distribution for the DNA translocation in a nanopore.

3.3.1. Charge model of the buffer solution. At room temperature, we assume that all KCl molecules in the electrolyte solution are fully dissociated. Hence, in the absence of external potential, there is an equal number of K^+ and Cl^- ions when the electrolyte solution is at equilibrium:

$$[K^+]_0 = [Cl^-]_0 = c \tag{1}$$

where c is the concentration of the buffer solution, which is assumed to be constant. See the appendix for details.

In the presence of an electrostatic potential $\phi(\vec{r})$, the ion concentrations in solution obey the Boltzmann statistics [23]:

$$[K^+](\vec{r}) = [K^+]_0 \exp\left(\frac{q\phi(\vec{r})}{kT}\right) \tag{2}$$

$$[Cl^-](\vec{r}) = [Cl^-]_0 \exp\left(-\frac{q\phi(\vec{r})}{kT}\right) \tag{3}$$

where T is temperature and k is Boltzmann constant. The virtual solid-state parameters used for the solution permit us to formulate a whole semiconductor model for the charge and electric potential.

3.3.2. Semiconductor charge model. In the solid-state material regions, the electron and hole concentrations are given by basic semiconductor physics theory [23]. In the Si layers we assume the donor doping concentration $N_d^+ = 2 \times 10^{20}$ cm^{-3}, so the carriers are degenerate, and their distribution follows the Fermi–Dirac distribution. The electron concentration $n(\vec{r})$ and the hole concentration $p(\vec{r})$ are given by [23]

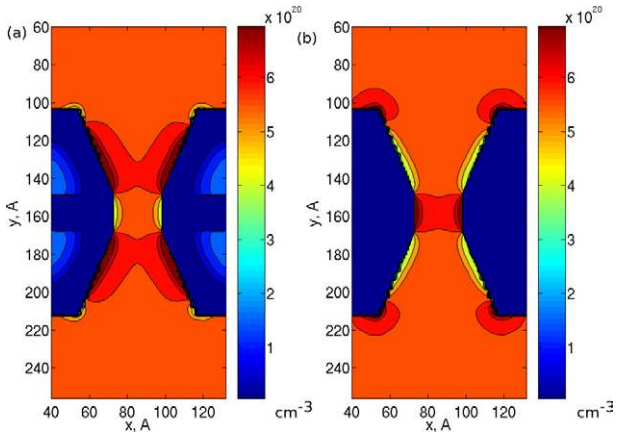

Figure 6. Contour plots of (a) negative charge and (b) positive charge in the structure and solution that are taken in the middle of the empty structure.

$$n(\vec{r}) = N_{\rm c}\frac{2}{\sqrt{\pi}}F_{1/2}\left(\eta_{\rm c}(\vec{r})\right) \tag{4}$$

$$p(\vec{r}) = N_{\rm v}\frac{2}{\sqrt{\pi}}F_{1/2}\left(\eta_{\rm v}(\vec{r})\right) \tag{5}$$

where $N_{\rm c}$ and $N_{\rm v}$ are the density of states in the conduction and valence bands of the solid-state material; $F_{1/2}$ is the 1/2 order Fermi–Dirac function, the parameters $\eta_{\rm c}(\vec{r})$ and $\eta_{\rm v}(\vec{r})$ are related to the local potential $\phi(\vec{r})$ by

$$\eta_{\rm c}(\vec{r}) = \frac{E_{\rm f} - E_{\rm c}(\vec{r})}{kT}, \qquad \text{with } E_{\rm c}(\vec{r}) = -q\phi(\vec{r}) - E_{\rm g} \tag{6}$$

$$\eta_{\rm v}(\vec{r}) = \frac{E_{\rm v}(\vec{r}) - E_{\rm f}}{kT}, \qquad \text{with } E_{\rm v}(\vec{r}) = -q\phi(\vec{r}) \tag{7}$$

where $E_{\rm c}(\vec{r})$ is the solid-state material conduction band edge profile and $E_{\rm v}(\vec{r})$ is the corresponding valence band edge profile; $E_{\rm g}$ is the band gap of the material; $E_{\rm f}$ is the Fermi level, which, because of the nature of the system, is assumed to be constant and is taken as our reference energy level.

To model the electrolyte/semiconductor interface we also use the conduction band offset between materials with respect to the Si:

$$\Delta E_c^{\rm SiO_2} = 3.2\ {\rm eV}, \qquad \Delta E_c^{\rm solution} = -0.3\ {\rm eV}. \tag{8}$$

This essential feature of the solid-state materials accounts for Fermi level pinning and band bending in the presence of the positive space charge inside the semiconductor and close to the interface. $\Delta E_c^{\rm SiO_2}$ is a measured value, whereas $\Delta E_c^{\rm solution}$ is a model parameter. The choice of its value does not affect the induced voltage dramatically.

We also include in our model a thin (2 Å) layer of negative charge at the surface of the semiconductor structure with the density of $N_{\rm surface} = 10^{21}$ cm^{-3}, resulting from the etching process [14]. While the density of this surface charge is not known precisely, the amplitude of the calculated voltage signal due to DNA translocation varies by 5% if the magnitude of the charge present on the surface of the nanopore is reduced to $N_{\rm surface} = 10^{10}$ cm^{-3}. The surface charge density value is selected to accommodate the experimental data [14]. In our treatment we do not consider the tunnelling current between the electrodes through the DNA.

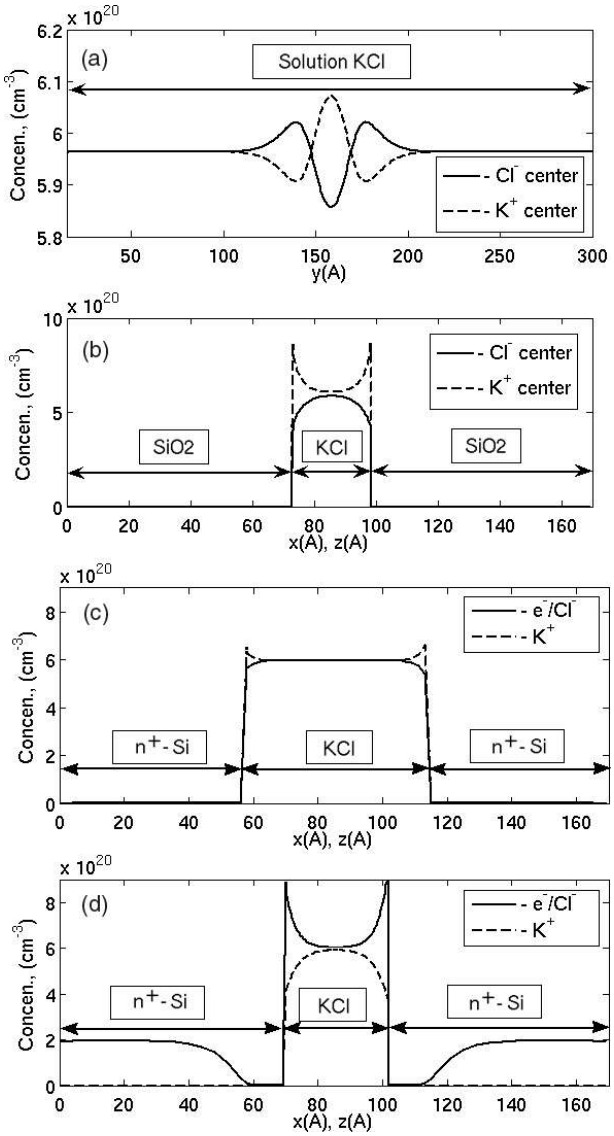

Figure 7. Concentrations of K^+ and Cl^- ions in the salt solution (a) along the pore central axis, $X_{\rm c}$ and (b) along a direction perpendicular to the pore axis and through the centre plane of the SiO_2 layer, $Y_{\rm c}$. Concentrations of electrons, Cl^- and K^+ in the device for two horizontal cross-sections, Y_1 (c) and Y_2 (d) (not through the pore centre). See figure 3 for definition of cross-sections.

3.3.3. Self-consistent scheme. The system under investigation consists of several material regions which are the Si and SiO_2 layers, and the buffer solution containing the DNA. The charge in different regions of the device originates from different sources. In the Si layers the charge comes from the doping ions, electrons and holes. The charge density in the solid-state regions is given by

$$\rho_{\rm solid-state}(\vec{r}) = q\left\{N_{\rm d}^+(\vec{r}) - N_{\rm a}^-(\vec{r}) + p(\vec{r}) - n(\vec{r})\right\} \tag{9}$$

where N_d^+ is the donor density, assumed to be fully ionized, and $N_{\rm a}^-(\vec{r})$ is the acceptor density, which is zero in our model.

In the buffer solution, contributions to the charge include the K^+ and Cl^- ions, along with the charge distribution on the DNA strand, $\rho_{\rm DNA}(\vec{r})$. The charge density of the solution is

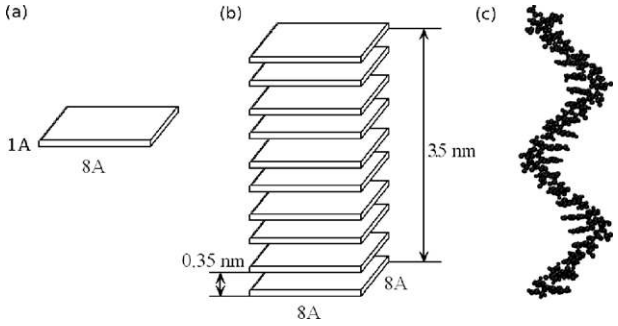

Figure 8. Three cases of different charge geometry that were simulated to obtain the voltage trace as a result of the charge translocation through the nanopore: (a) point charge, (b) linear charge and (c) helical fragment of a single-stranded DNA.

then

$$\rho_{\text{solution}}(\vec{r}) = q\left\{[\text{K}^+](\vec{r}) - [\text{Cl}^-](\vec{r})\right\} + \rho_{\text{DNA}}(\vec{r}). \qquad (10)$$

Each material is characterized by its relative permittivity, i.e., $\epsilon_{\text{Si}} = 11.7$, $\epsilon_{\text{SiO}_2} = 3.9$. For the buffer solution we chose the dielectric constant to be that of water, i.e. $\epsilon_{\text{solution}} = 78$. We also assume the same value inside the nanopore ($\epsilon_{\text{pore}} = 78$), although due to the size of the pore, the dielectric constant may exhibit significant local variation [24]: the relative permittivity inside the pore may vary from 78 to 1 depending on whether or not the water is completely excluded from the pore during the DNA translocation. The exclusion of water may have a dramatic effect on the signal and therefore we are motivated to study translocations in narrow (∼1 nm) diameter pores.

Poisson's equation,

$$\vec{\nabla}\cdot\left(\epsilon(\vec{r})\vec{\nabla}\phi(\vec{r})\right) = -\rho(\vec{r}), \qquad (11)$$

is solved self-consistently by a multigrid method [25] on the whole volume of the simulated structure with the following boundary conditions: Dirichlet boundary conditions at the top and the bottom bias gate regions ($\phi_{\text{top-gate}} = \phi_{\text{bottom-gate}} = 0$). Neumann boundary conditions were applied for other regions.

The self-consistent three-dimensional Poisson solver is set up as follows: upon entering the initial guess charge distribution, i.e., DNA charge plus electrolyte ionic charge, the numerical solution starts from solving the Poisson equation to obtain the potential distribution. The local potential is then substituted into the materials constructive equations to obtain a corresponding local charge concentration (ionic concentration in the buffer solution region, electrons in other regions). The charge concentration is then inserted back into the Poisson equation and the new potential distribution is calculated. The procedure is repeated for every input charge distribution until convergence is obtained. For the potential, the convergence tolerance was 1 μV.

Due to the DNA strand translocation through the nanopore, the DNA charge distribution is position-dependent. Therefore, in future work we plan use 'snapshots' of the DNA charge distribution profile provided by the MD simulation as input into our 3D self-consistent Poisson solver (for the sake of simplicity while testing the model, here we use only one initial snapshot which we translocate rigidly through the pore). In other words, the MD simulation provides the DNA charge distribution snapshot(s) to the Poisson solver. Following this, we calculate the corresponding quasi-static charge and potential distributions in the device and the surrounding solution.

In order to calculate the voltage induced on the Si electrodes due to a charge translocation we average the potential over the circular perimeter of the pore at the intersection of the SiO_2 and Si layers. Thus, we record the potential at the nearest possible distance between the electrode and the DNA. In this way we obtain two potential values, one for the upper (*cis*) electrode and one for the lower (*trans*) electrode. We subtract the corresponding values of the potential for the empty nanopore (pore without translocating charge) to obtain the potential difference induced on the electrodes by the translocating charge.

Our multi-scale/multi-material approach methodology is outlined in figure 5 in the form of a chart diagram.

4. Results and discussion

In this section we characterize the modelled device, as well as study the translocation of the negative test charge, two linear sequences of charges and a ssDNA.

4.1. Empty structure

We begin our analysis with the characterization of the structure immersed in KCl solution without translocating molecule in the pore (empty nanopore). The contour plots of the concentrations of electrons in the device, and concentrations of Cl^- and K^+ ions in the solution, are shown in figures 6(a) and (b) with a bulk concentration of 1 M. In the device region the surface is mostly depleted from electrons owing to the presence of negative surface charges, leaving only the positive fixed charge of ionized donors. The centre layer always stays void of carriers since it is SiO_2, a dielectric. Our data show an accumulation of K^+ ions in the centre of the pore in the electrolyte region with a reduction of Cl^- ions, which is due to the presence of negative surface charges. However, on the slanted sides of the pore, despite the negative charge, there is an inversion of ion concentration (figure 7(a)) with a significant increase of Cl^- ion concentration even at the interface. This effect is attributed to the presence of the depletion region in the n^+-doped semiconductor where the effect of the positive charge of the fixed ionized donors on the ions in the solution is enhanced by the funnel geometry of the Si layers. Far from the nanopore, the KCl concentration is 6×10^{20} ions cm^{-3}, which corresponds to 1 M (as assumed).

Figure 7(a) shows the distribution of K^+ and Cl^- ions in the solution along the pore central axis (X_c on figure 3). We observe the accumulation of K^+ ions and the corresponding reduction of Cl^- ions in the middle of the pore. While the inversion of ion concentrations occurs on each side of the nanopore centre, it can be seen in figure 7(b) that K^+ ions also accumulate at the pore perimeter, forming the expected 'double layer', whereas the Cl^- ion concentration is larger in the pore centre compared to its concentration at the pore perimeter.

The concentrations of electrons in the device for two horizontal cross-sections (not through the pore centre) are

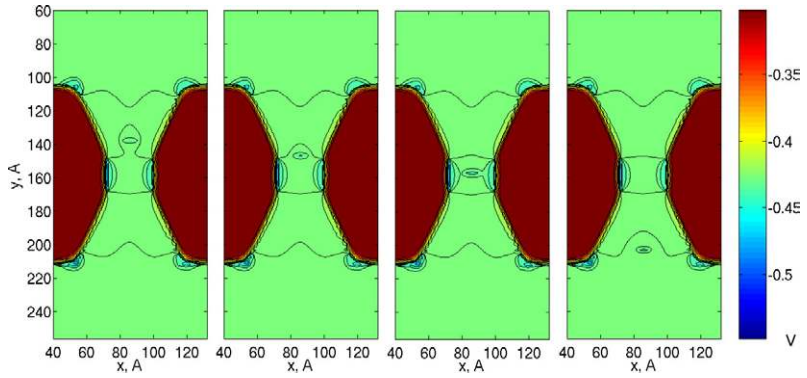

Figure 9. Several potential contours taken in the middle of the nanopore illustrate the test charge movement through the nanopore. The positions of the test charge centre are $y = 137$, 147, 157 and 177 Å (from left to right).

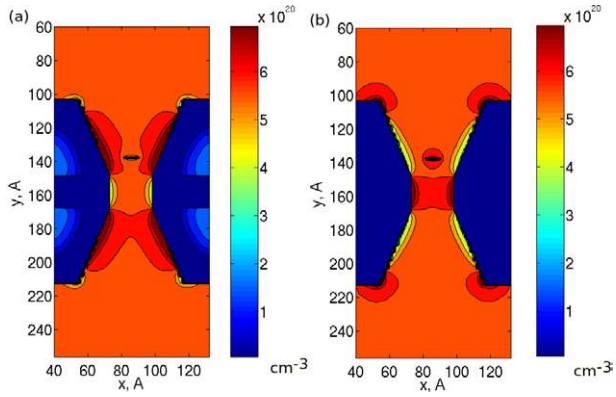

Figure 10. (a) Cl^- ion and (b) K^+ ion distribution in the surrounding salt solution in the presence of the test charge.

shown in figure 7(c) for the Y_1 cross-section and figure 7(d) for the Y_2 cross-section (cf figure 3). The former (figure 7(c)) shows the wide extension of the depletion region in the Si layer while the latter (figure 7(d)) shows only a thin depletion layer remaining near the surface of the pore with the inverted ion concentrations at the interface as one moves closer to the SiO_2 layer.

We can estimate the number of ions in the volume of the nanopore as $N_{\text{pore}} = CV_{\text{pore}}$, where $C = 1$ M is the average electrolyte solution concentration in the nanopore (see figure 7) as a cylinder of height $h = 2$ nm with radius $R_{\text{pore}} = (2.5/2)$ nm. Thus, $N_{\text{pore}} = 7.53$. This value compares very well with the average number of potassium and chlorine ions in the pore during the course of molecular dynamics simulation, where there are 5–10 potassium and chlorine ions on average present in the pore [16].

The charge on the surface of the pore was calculated as $[N_{\text{surface}} \times 2\ \text{Å}]\ [h \times 2\pi R_{\text{pore}}]\text{e}^- \approx 3.14\text{e}^-$, which is comparable to the value inferred from the measured electrolytic conductivity [14]. This number is consistent with the number of ions in the pore, so that there is an overall neutrality of the region. For comparison, a DNA carries an excessive charge of 1e^- per base and several bases may be trapped between the electrodes at any particular time during a DNA translocation.

4.2. Test charge translocation

In order to assess the magnitude of the voltage response on the capacitor plates, and to calibrate our model, we first simulate the translocation of a negative test charge of $-1e$ through the nanopore to mimic the charge of a DNA base distributed on a slab of $8 \times 8 \times 1$ Å^3 with excluded water and ions from the slab (figure 8(a)). The test charge proceeds by steps of 1 Å along the axis of the nanopore, while we compute the electrostatic potential in the device for each charge position.

Figure 9 illustrates the point charge translocation as contour plots of the electrostatic potential profile shown for four different positions of the test charge in a 1.0 M KCl electrolyte solution. The major perturbation of the potential in response to the varying position of the test charge occurs inside the narrowest part of the nanopore, while the solid-state regions are less affected. This is due to the large difference between the dielectric constant of the electrolyte ($\epsilon_{\text{solution}} = 78$) and of the solid-state materials ($\epsilon_{\text{Si}} = 11.7$ and $\epsilon_{\text{SiO}_2} = 3.9$) as well as because of the screening by the mobile ions. Despite the efficient electrolyte screening, a small voltage signal of the order of 100 μV is recorded on the two electrodes.

Figure 10 illustrates the concentration of positive and negative ions around the test charge. In particular, it shows the repulsion of negative ions from and attraction of positive ions to the test charge.

As seen in figures 11(a) and (b), the peak voltage occurs at positions of the test charge corresponding to its closest proximity to each electrode. Hence, at charge position $y = 148$ Å, the test charge is just in front of the narrowest part of the upper Si layer, while a similar situation occurs at charge position $y = 167$ Å for the lower electrode. We evaluate the fluctuation in the recorded signal level by varying the position of the charge in the pore with the centre of the charge lying in plane with the electrode. The average calculated signal is 100 μV for the test charge on the central axis of the pore and at the nearest distance to the electrode, as seen in figures 11(a) and (b). However, the amplitude of the signal increases to ~300–400 μV when the charge is moved closer to the electrode's wall. Thus, the magnitude of the simulated signal is encouraging since it is significantly above the resolution of conventional charge detectors.

We also note that the signals on the upper electrode and lower electrode are symmetric with respect to the coordinate

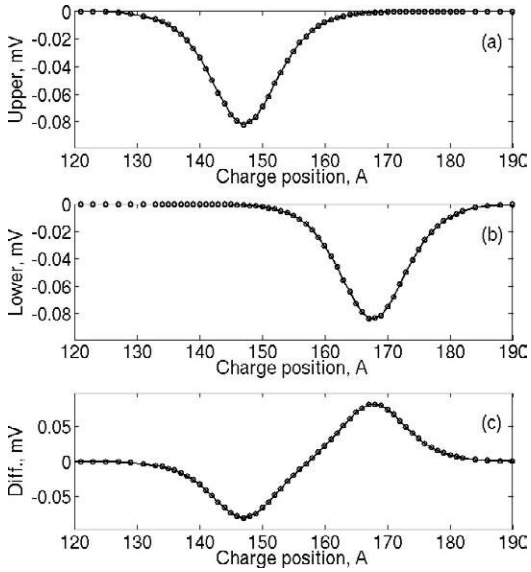

Figure 11. Voltage signals on the two electrodes for the single negative point charge passing through the nanopore: (a) upper electrode voltage signal, (b) lower electrode voltage signal, and (c) voltage difference between (a) and (b). The horizontal axis reflects the position of the test charge centre in the pore.

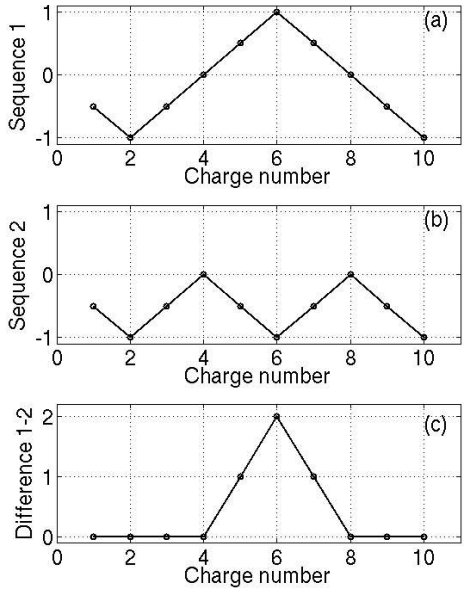

Figure 12. Two modelled linear charge sequences with individual charge values varying from −1e to +1e (a), and from −1e to 0 (b); and the difference between the two sequences (c).

$y = 157.5$ Å (at this coordinate the test charge is at the centre of the nanopore) as a result of the pore symmetry and the uniform motion of the charge through the nanopore.

Figure 11(c) shows the potential difference between the two electrodes as a function of the test charge position. The trace voltage signal is anti-symmetric with respect to the charge position $y = 157.5$ Å at which the recorded voltage is zero, as it should be, due to the pore symmetry.

4.3. Translocation of a linear sequence of charge

In order to evaluate the capacitor resolution for detection of a DNA base sequence we simulate step-by-step the translocation of two different sequences of linear charges through the nanopore and compute the voltage signal on the electrodes. For this purpose we consider two sequences of ten charges: the first sequence is '−0.5e −1.0e −0.5e 0.0e +0.5e +1.0e +0.5e 0.0e −0.5e −1.0e' (figure 12(a)) and the second sequence is '−0.5e −1.0e −0.5e 0.0e −0.5e −1.0e −0.5e 0.0e −0.5e −1.0e' (figure 12(b)), translocating along the nanopore axis from top to bottom, with the end of each sequence entering the nanopore first. Each linear sequence consists of ten flat slabs carrying the assigned charge and separated by 0.35 nm to mimic a DNA strand. The linear charge geometry is shown in figure 8(b). The total length of the sequence is about 3.5 nm. Water and ions are excluded from the slabs.

Figures 13(a) and (b) show the voltage signals obtained on the Si electrodes for the rigid translocation of the first and the second charge sequences, respectively, starting from a position where the first charge of the sequence is just above the SiO_2 nanopore to a position where the last charge of the sequence is below it. As in the case of the test charge, the sequence proceeds rigidly through the pore by steps of

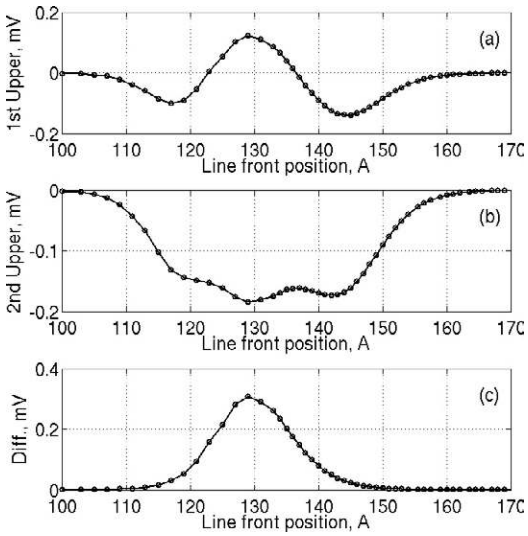

Figure 13. Recorded voltage signals of the two line charge sequences passing through the nanopore: (a) upper electrode voltage signal for the first sequence, (b) upper electrode voltage signal for the second sequence, and (c) voltage difference between (a) and (b). The horizontal axis shows the position of the line charge front in the pore. The lower electrode trace is similar to the upper electrode trace for the corresponding linear sequence (not shown).

1.0 Å. As expected, the voltage response for each set is not proportional to the total charge in the sequence, but reflects the convoluted effect of the position of individual charges in the sequence when passing close to the nearest electrode. Moreover, unlike the case of the single test charge, the signal is not symmetric with respect to the 'zero-voltage' point, since the charges are not distributed symmetrically around the centre of mass of the sequence. In the same context, the 'zero-voltage' point is different for the two sequences.

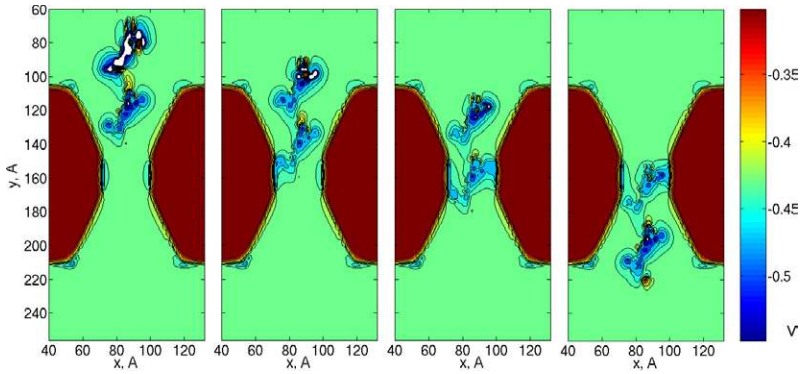

Figure 14. Potential contours taken in the middle of the nanopore for the single-stranded DNA translocating through the nanopore.

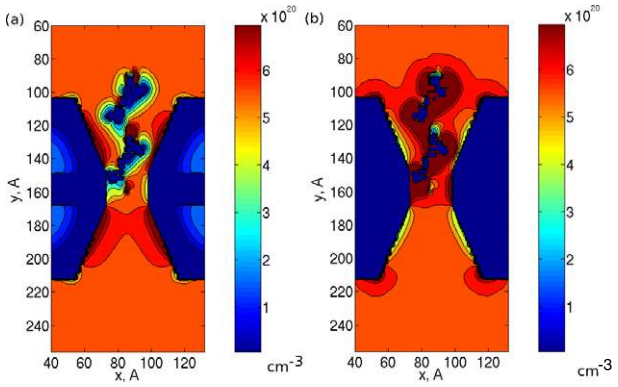

Figure 15. (a) Cl^- ion and (b) K^+ ion distribution in the surrounding salt solution in the presence of the DNA.

The first sequence consists of positive and negative charges while the second sequence consists of only negative charges. As a result, positive and negative voltages are recorded while the first sequence translocates the nanopore (figure 13(a)); however, only a negative voltage is recorded during the translocation of the second sequence (figure 13(b)).

Figure 13(c) shows the difference between the signals of the two sequences. As can be seen, the sequences are distinguishable within 0.3 mV with a characteristic signal shape. Also, as the beginning and the end of two sequences are identical, only the middle part of the trace voltage difference is not zero (see figure 11(c) for the difference between two charge sequences). When comparing the charge sequences in figures 11(a)–(c) with the recorded voltage traces in figures 13(a)–(c) one observes a remarkable similarity of both signals.

4.4. Translocation of a single-stranded DNA

We simulated then the translocation of a 20-nucleotide long poly$(dC)_{20}$ ssDNA molecule in a helical conformation [2] (see figure 8(c)) through the nanopore, computing the voltage signal induced on the Si electrodes. As described above, we extract the DNA charge distribution from molecular dynamics simulation by taking into account every atom's contribution of the DNA strand (see section 3) and map the charge distribution into the Poisson solver. For this purpose, every atom's charge on the DNA strand is distributed over a sphere of 3 Å in diameter, but solution charge was excluded from this volume as it was also excluded in the two previous cases.

Figure 14 shows the potential contours in the middle of the pore for four different DNA positions as it proceeds along the pore axis. The DNA translocates parallel to the axis on the nanopore and is slightly off the nanopore centre, a situation which is likely to happen in a real experimental set-up. Figure 14 shows the merging of equipotential caused by the DNA molecule with the solid-state nanopore which induces a potential variation in the Si layers.

Figure 15(a) depicts the increased concentration of positive ions around the DNA, which is dominantly negatively charged, while figure 15(b) shows the repulsion of negative ions from the molecule. We note that K^+ ions are mainly localized around the negatively charged backbone of the molecule. There is a mix of K^+ and Cl^- ions in the surrounding DNA bases solution. Of interest is also the change in ion concentrations caused by the DNA when compared to the concentrations in the empty pore as shown in figure 6.

Figure 16 shows the electrode voltage signal obtained from the rigid translocation of the DNA molecule through the nanopore. One notices the magnitude of the signal of the order of 10 mV, which is much larger than in the case of the linear chain due to the more densely packed charge on the DNA chain. Also, owing to the rigid translocation, the signal at the lower electrode is shifted by 2 nm relative to the upper electrode signal. From the non-zero voltage trace one can conclude that the translocated DNA is about 75 Å long. In addition, the recorded signal reflects the DNA strand structure and conformation with distinguishable features that are about 4 Å apart (compared to 3.4 Å separation between the bases on a DNA strand). This implies that it is possible to identify individual bases as they pass by the electrodes. However, the off-centre translocation of modelled DNA helix does not allow one to identify all of the bases in the strand, but only those that come close to the electrodes. Indeed, as the translocating DNA consists of 20 identical cytosine bases, the variation in the recorded signal between 10 and 15 mV can be looked at as the variation due to *positional noise* of a single cytosine base in the pore, which we estimate to be ∼2–3 mV.

Narrower nanopores would constrict the translocating molecules to smaller volume and, thereby, reduce the distance between nucleotides and Si electrodes, resulting in larger and

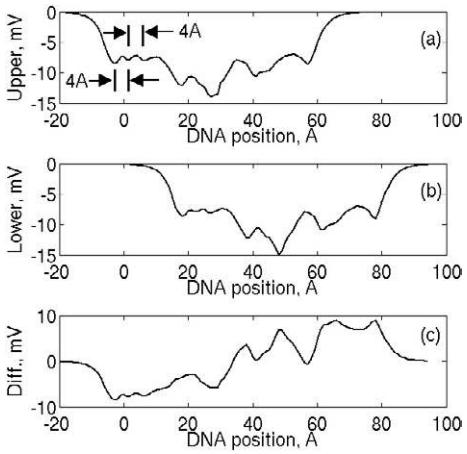

Figure 16. Voltage signals on the two electrodes for a single-stranded DNA poly$(dC)_{20}$ passing through the nanopore: (a) upper electrode voltage signal, (b) lower electrode voltage signal, and (c) voltage difference between (a) and (b). The horizontal axis shows the position of the DNA front in the pore.

higher resolution signals. Also, it is well known that, in electrolytic solutions, each DNA base is characterized by a specific dipole moment, which is electrically identifiable. Here again, the constriction of the DNA to a very narrow pore could be used to reduce the stochastic orientation of dipole moment resulting from molecular dynamics, thus considerably lowering the conformational noise of the bio-molecule.

5. Conclusion

We performed a three-dimensional multi-scale/multi-material numerical simulation of the quasi-electrostatic characteristics of a novel solid-state nano-biophysical device which can be used as a DNA detector. The simulation demonstrates the possibility of a nanopore device to function as a DNA detector. In particular, we show that the DNA translocation causes the electrodes' voltage to exhibit changes in excess of 10 mV that can be recorded experimentally. From the recorded voltage trace we also show the possibility to measure DNA length and observe fine features that correspond to single nucleotides.

These experiments and simulations are only the first step in our exploration of the nanopore–capacitor mechanism of DNA single molecule electrical sequencing. We have carried out numerous molecular dynamics simulations of DNA translocation through the pore [16]. However, only one DNA snapshot was analysed with respect to the electric response of the nanopore and was presented in this manuscript. Several other DNA snapshots that were also analysed (but not presented) produced similar results. The analysis of more realistic stochastic DNA translocation is a subject of our current research. Also, in future work we plan to incorporate the calculated potential profile into the molecular dynamics simulation to obtain the feedback from induced potential on the DNA motion through the pore.

Acknowledgments

This work is supported by the ITR-NSF Grant No. NSF-FCCR0121616, the NIRT-NSF Grant No. NSFCCR02-10843, the Darpa Grant No. 392FA9550-04-1-0214, and NIH grant ROI-HG003713; computer time was provided through National Allocation Committee grant MCA05S028S and MCA93S028.

Appendix. Ionic concentrations

The ionic concentrations in KCl electrolyte solution are similar to electron and hole concentrations in an intrinsic semiconductor. Because of this similarity, we can consider the K^+Cl^- electrolytic solution as an intrinsic semiconductor and introduce virtual semiconductor parameters, i.e., a virtual energy band gap E_{geff}, virtual density states of K^+ ions and Cl^- ions, N_{K^+} and N_{Cl^-}, and virtual effective masses, $m^*_{K^+}$ and $m^*_{Cl^-}$ for potassium and chlorine ions, respectively [26]. With these virtual parameters, we can calculate the ion concentrations of the electrolytic solution as follows:

$$[K^+]_0 = [Cl^-]_0 = \sqrt{N_{K^+} N_{Cl^-}} \exp\left(-\frac{E_{\text{geff}}}{2kT}\right) \qquad \text{(A.1)}$$

where $[K^+]_0$ and $[Cl^-]_0$ are the bulk ion concentration, and the virtual density of states N_{K^+} and N_{Cl^-} are given by

$$N_{K^+} = 2\left(\frac{m^*_{K^+} kT}{2\pi\hbar^2}\right) \qquad N_{Cl^-} = 2\left(\frac{m^*_{Cl^-} kT}{2\pi\hbar^2}\right). \qquad \text{(A.2)}$$

References

[1] Kasianowicz J J, Brandin E, Branton D and Deamer D W 1996 Characterization of individual polynucleotide molecules using a membrane channel *Proc. Natl Acad. Sci. USA* **93** 13770–3

[2] Saenger W 1983 *Principles of Nucleic Acid Structure* (New York: Springer)

[3] Song L *et al* 1996 Structure of staphylococcal alpha-hemolysin, a heptameric transmembrane pore *Science* **274** 1859–65

[4] Akenson M, Branton D, Kasianowicz J J, Brandin E and Deamer D W 1999 Microsecond timescale discrimination among polycytidylic acid, polyadenylic acid, and polyuridylic acid as homopolymers or as segments within single RNA molecules *Biophys. J.* **77** 3227–33

[5] Meller A, Nivon L, Brandin E, Golovchenko J and Branton D 2000 Rapid nanopore discrimination between single polynucleotide molecules *Proc. Natl Acad. Sci. USA* **97** 1079–84

[6] Deamer D W and Akeson M 2000 Nanopores and nucleic acids: prospects for ultrarapid sequencing *Trends Biotech.* **18** 147–51

[7] Vercoutere W, Winters-Hilt S, Olsen H, Deamer D, Haussler D and Akeson M 2001 Rapid discrimination among individual DNA hairpin molecules at single-nucleotide resolution using an ion channel *Nat. Biotech.* **19** 248–52

[8] Meller A, Nivon L and Branton D 2001 Voltage-driven DNA translocations through a nanopore *Phys. Rev. Lett.* **86** 3435–8

[9] Meller A and Branton D 2002 Single molecule measurements of DNA transport through a nanopore *Electrophoresis* **23** 2583–91

[10] Deamer D W and Branton D 2002 Characterization of nucleic acids by nanopore analysis *Acc. Chem. Res.* **35** 817–25

[11] Li J, Gershow M, Stein D, Brandin E and Golovchenko J A 2003 DNA molecules and configurations in a solid-state nanopore microscope *Nat. Mater.* **2** 611–5

[12] Heng J B *et al* 2003 The detection of DNA using a silicon nanopore *IEDM Tech. Digest* 767–70
[13] Heng J B, Ho C, Kim T, Timp R, Aksimentiev A, Grinkova Y V, Sligar S, Schulten K and Timp G 2004 Sizing DNA using an artificial nanopore *Biophys. J.* **87** 2905–11
[14] Ho C, Qiao R, Heng J B, Chatterjee A, Timp R J, Aluru N R and Timp G 2005 Electrolytic transport through a synthetic nanometer-diameter pore *Proc. Natl Acad. Sci.* **102** 10445–50
[15] Storm A J, Chen J H, Ling X S, Zandbergen H W and Dekker C 2003 Fabrication of solid-state nanopores with single-nanometer precision *Nat. Mater.* **2** 537–40
[16] Aksimentiev A, Heng J B, Timp G and Schulten K 2004 Microscopic kinetics of DNA translocation through synthetic nanopores *Biophys. J.* **87** 2086–97
[17] Heng J, Aksimentiev A, Ho C, Dimitrov V, Sorsch T, Miner J, Mansfield W, Schulten K and Timp G 2005 Beyond the gene chip *Bell Labs Tech. J.* **10** 5–22
[18] Heng J, Aksimentiev A and Timp G 2005 The electromechanics of DNA in a nanopore *Biophys. J.* at press
[19] Heng J, Aksimentiev A, Ho C, Marks P, Grinkova Y, Sligar S, Schulten K and Timp G 2005 Stretching DNA using the electric field in a synthetic nanopore *Nano Lett.* **5** 1883–8
[20] Phillips J C, Braun R, Wang W I, Gumbart J, Tajkhorshid E, Villa E, Chipote C, Skeel R D, Kale L and Schulten K 2005 Scalable molecular dynamics with NAMD *J. Comput. Chem.* **26** 1781–802
[21] Cornell W D, Cieplak P, Bayly C I, Gould I R, Merz K M, Ferguson D M, Spellmeyer D C, Fox T, Caldwell J W and Kollman P A 1995 Second generation force filed for the simulation of proteins, nucleic acids, and organic molecules *J. Am. Chem. Soc.* **117** 5179–97
[22] Wendel J A and Goddard W A 1992 The Hessian biased force-field for silicon nitride ceramics: predictions of thermodynamic and mechanical properties for a- and b-Si_3N_4 *J. Chem. Phys.* **97** 5048–62
[23] Sze S M 1981 *Physics of Semiconductor Devices* (New York: Wiley)
[24] Sansom M S, Smith G R, Adcock C and Biggin P C 1997 The dielectric properties of water within model transbilayer pores *Biophys. J.* **73** 2404–15
[25] Press W H, Teukolsky S A, Vetterling W T and Flannery B P 2001 *Numerical Recipes in Fortran 77* (Cambridge: Cambridge University Press)
[26] Muller R S, Kamins T I and Chan M 2003 *Device Electronics for Integrated Circuits* (New York: Wiley)